Supplementary Information (SI) for Lab on a Chip.
This journal is © The Royal Society of Chemistry 2025

Supporting Information

Realization of Rapid Diabetic Retinopathy Screening with Lipocalin 1 in Tear Using Enhanced Immunofluorescence Photonic Crystal Microchip

Kullaphat Nitayachat [†1], Dhrubajyoti Das [†1], Pei-Yi Chen [1], Sheng-Min Hsu [2], Jhih-Cheng Wang [3,4,5]** and Han-Sheng Chuang [1,6]*

[1]Department of Biomedical Engineering, National Cheng Kung University, Tainan 701, Taiwan
[2]Department of Ophthalmology, National Cheng Kung University Hospital, College of Medicine, National Cheng Kung University, Tainan 701, Taiwan
[3]Division of Urology, Department Surgery, Chi Mei Medical Center, Tainan, Taiwan
[4]Department of Electrical Engineering, Southern Taiwan University of Science and Technology, Tainan, Taiwan
[5]School of Medicine, College of Medicine, National Sun Yat-sen University, Kaohsiung, Taiwan
[6]Medical Device Innovation Center, National Cheng Kung University, Tainan 701, Taiwan

* Corresponding author: oswaldchuang@mail.ncku.edu.tw
** Co-Corresponding author: tratadowang@gmail.com

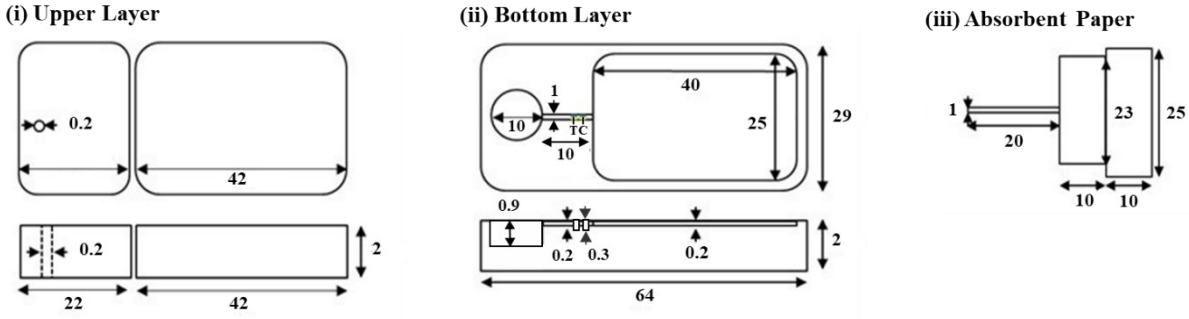

Fig. S1 Detailed dimensions of the microfluidic chip components. (i) Upper layer including the sample loading inlet. (ii) Bottom layer showing the circular groove, microfluidic channel, and absorbent paper reservoir. (iii) Dimensions of the absorbent paper. (unit: mm).

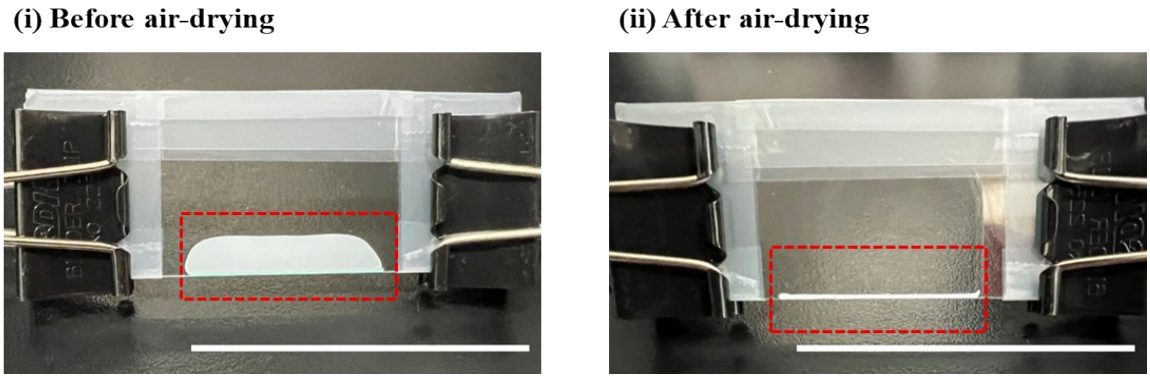

Fig. S2 Images of PhC fabrication. (i) A concentrated PMMA nanoparticle suspension was applied onto a hydrophobically treated glass slide and secured using two binder clips. The red dotted rectangle highlights the suspension spread on the slide. (ii) Formation of the PhC at the edge of the slides after air-drying at room temperature (25 °C) for 24 hours. The red dotted rectangle indicates the region where the PhC structure is visibly formed (scale bar: 5 cm).

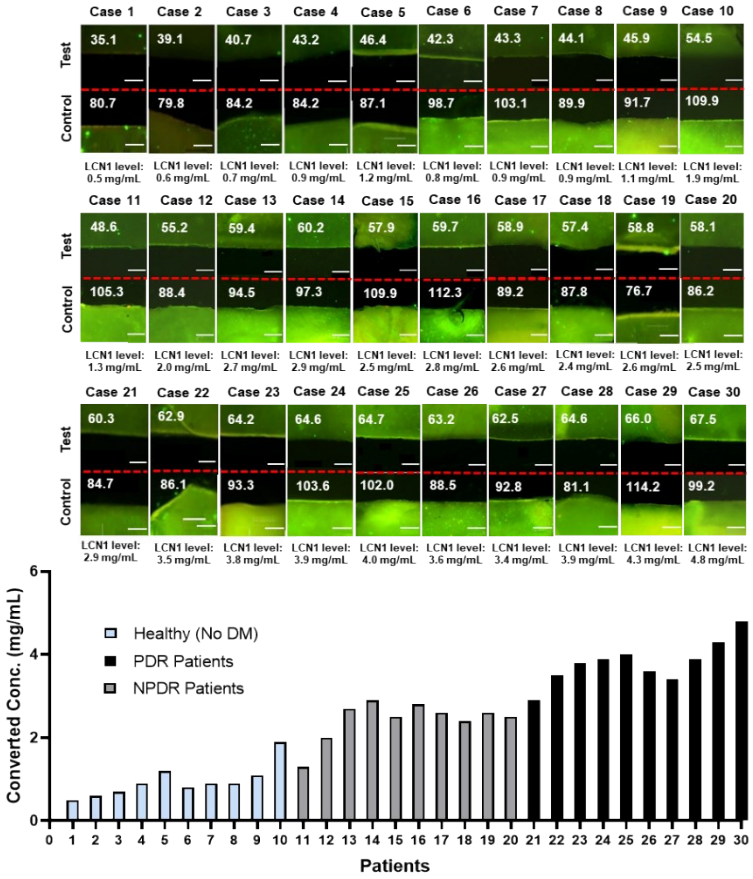

Fig. S3 Fluorescence images and calculated LCN-1 levels in tear samples. Shown are healthy controls (cases 1–10), NPDR patients (cases 11–20), and PDR patients (cases 21–30). The bar graph summarizes converted LCN-1 concentrations for all cases (n = 30).

S1. Sensitivity, specificity and accuracy calculation:

For the clinical validation study, sensitivity, specificity, and accuracy were determined using standard definitions based on true positive, true negative, false positive, and false negative classifications. All metrics were computed using receiver operating characteristic (ROC) curve analysis in GraphPad Prism software, which automatically calculates the area under the curve (AUC), optimal cut-off value, and diagnostic performance indices from clinical data.

$$Sensitivity = \frac{True\ Positives}{True\ Positives + False\ Negatives}$$

$$Specificity = \frac{True\ Negutives}{True\ Negatives + False\ Positives}$$

$$Accuracy = \frac{True\ Positives + True\ Negatives}{Total\ Number\ of\ Samples}$$

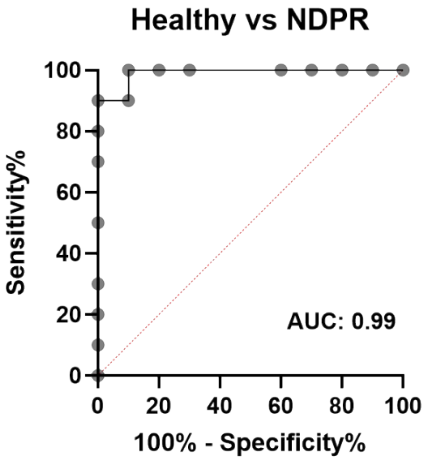

True Positive (TP) = 10 → NPDR patients correctly classified as NPDR
False Negative (FN) = 0 → NPDR patient misclassified as Healthy
True Negative (TN) = 9 → Healthy patients correctly classified as Healthy
False Positive (FP) = 1 → Healthy patient misclassified as NPDR

$$Accuracy = \frac{TP + TN}{Total} = \frac{10 + 9}{20} = \frac{19}{20} = 95\%$$

		Sensitivity%	95% CI	Specificity%	95% CI	Likelihood ratio
1	> 0.5500	100.0	72.25% to 100.0%	10.00	0.5129% to 40.42%	1.111
2	> 0.6500	100.0	72.25% to 100.0%	20.00	3.554% to 50.98%	1.250
3	> 0.7500	100.0	72.25% to 100.0%	30.00	10.78% to 60.32%	1.429
4	> 0.8500	100.0	72.25% to 100.0%	40.00	16.82% to 68.73%	1.667
5	> 1.000	100.0	72.25% to 100.0%	70.00	39.68% to 89.22%	3.333
6	> 1.150	100.0	72.25% to 100.0%	80.00	49.02% to 96.45%	5.000
7	> 1.250	100.0	72.25% to 100.0%	90.00	59.58% to 99.49%	10.00
8	> 1.600	90.00	59.58% to 99.49%	90.00	59.58% to 99.49%	9.000
9	> 1.950	90.00	59.58% to 99.49%	100.0	72.25% to 100.0%	
10	> 2.200	80.00	49.02% to 96.45%	100.0	72.25% to 100.0%	
11	> 2.450	70.00	39.68% to 89.22%	100.0	72.25% to 100.0%	
12	> 2.550	50.00	23.66% to 76.34%	100.0	72.25% to 100.0%	
13	> 2.650	30.00	10.78% to 60.32%	100.0	72.25% to 100.0%	
14	> 2.750	20.00	3.554% to 50.98%	100.0	72.25% to 100.0%	
15	> 2.850	10.00	0.5129% to 40.42%	100.0	72.25% to 100.0%	

Fig. S4. Receiver Operating Characteristic (ROC) curve analysis for distinguishing Healthy vs NPDR groups based on tear LCN-1 fluorescence intensity. The ROC curve was generated using GraphPad Prism software, with true positive (TP), false negative (FN), true negative (TN), and false positive (FP) classifications derived from clinical sample results. The highlighted yellow line indicates the optimal cut-off point selected by the software, corresponding to the highest combined sensitivity (100%) and specificity (90%). The calculated accuracy was 95% (19 correct classifications out of 20 samples).

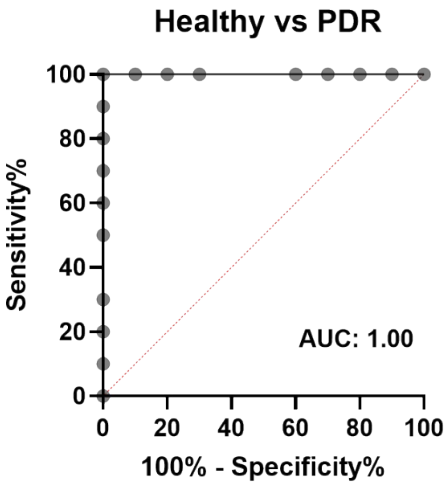

True Positive (TP) = 10 → PDR patients correctly classified as PDR
False Negative (FN) = 0 → PDR patients misclassified as Healthy
True Negative (TN) = 10 → Healthy patients correctly classified as Healthy
False Positive (FP) = 0 → Healthy patients misclassified as PDR

$$Accuracy = \frac{TP + TN}{Total} = \frac{10 + 10}{20} = \frac{20}{20} = 100\%$$

	Sensitivity%	95% CI	Specificity%	95% CI	Likelihood ratio
> 0.5500	100.0	72.25% to 100.0%	10.00	0.5129% to 40.42%	1.111
> 0.6500	100.0	72.25% to 100.0%	20.00	3.554% to 50.98%	1.250
> 0.7500	100.0	72.25% to 100.0%	30.00	10.78% to 60.32%	1.429
> 0.8500	100.0	72.25% to 100.0%	40.00	16.82% to 68.73%	1.667
> 1.000	100.0	72.25% to 100.0%	70.00	39.68% to 89.22%	3.333
> 1.150	100.0	72.25% to 100.0%	80.00	49.02% to 96.45%	5.000
> 1.550	100.0	72.25% to 100.0%	90.00	59.58% to 99.49%	10.00
> 2.400	100.0	72.25% to 100.0%	100.0	72.25% to 100.0%	
> 3.150	90.00	59.58% to 99.49%	100.0	72.25% to 100.0%	
> 3.450	80.00	49.02% to 96.45%	100.0	72.25% to 100.0%	
> 3.550	70.00	39.68% to 89.22%	100.0	72.25% to 100.0%	
> 3.700	60.00	31.27% to 83.18%	100.0	72.25% to 100.0%	
> 3.850	50.00	23.66% to 76.34%	100.0	72.25% to 100.0%	
> 3.950	30.00	10.78% to 60.32%	100.0	72.25% to 100.0%	
> 4.150	20.00	3.554% to 50.98%	100.0	72.25% to 100.0%	
> 4.550	10.00	0.5129% to 40.42%	100.0	72.25% to 100.0%	

Fig. S5. Receiver Operating Characteristic (ROC) curve analysis for distinguishing Healthy vs PDR groups based on tear LCN-1 fluorescence intensity. The ROC curve was generated using GraphPad Prism software, with TP, FN, TN, and FP classifications derived from clinical sample results. The highlighted yellow line indicates the optimal cut-off point selected by the software, corresponding to the highest combined sensitivity (100%) and specificity (100%). The calculated accuracy was 100% (20 correct classifications out of 20 samples).

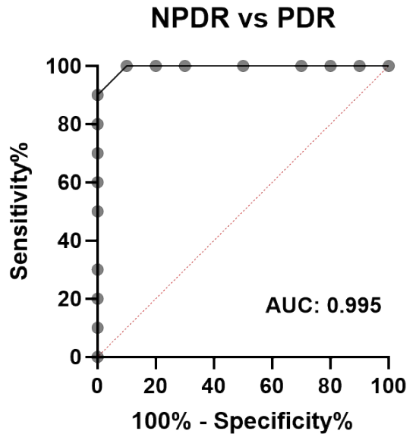

True Positive (TP) = 10 → PDR patients correctly classified as PDR
False Negative (FN) = 0 → PDR patients misclassified as NPDR
True Negative (TN) = 9 → NPDR patients correctly classified as NPDR
False Positive (FP) = 1 → NPDR patients misclassified as PDR

$$Accuracy = \frac{TP + TN}{Total} = \frac{10 + 9}{20} = \frac{19}{20} = 95\%$$

	Sensitivity%	95% CI	Specificity%	95% CI	Likelihood ratio
> 1.650	100.0	72.25% to 100.0%	10.00	0.5129% to 40.42%	1.111
> 2.200	100.0	72.25% to 100.0%	20.00	3.554% to 50.98%	1.250
> 2.450	100.0	72.25% to 100.0%	30.00	10.78% to 60.32%	1.429
> 2.550	100.0	72.25% to 100.0%	50.00	23.66% to 76.34%	2.000
> 2.650	100.0	72.25% to 100.0%	70.00	39.68% to 89.22%	3.333
> 2.750	100.0	72.25% to 100.0%	80.00	49.02% to 96.45%	5.000
> 2.850	100.0	72.25% to 100.0%	90.00	59.58% to 99.49%	10.00
> 3.150	90.00	59.58% to 99.49%	100.0	72.25% to 100.0%	
> 3.450	80.00	49.02% to 96.45%	100.0	72.25% to 100.0%	
> 3.550	70.00	39.68% to 89.22%	100.0	72.25% to 100.0%	
> 3.700	60.00	31.27% to 83.18%	100.0	72.25% to 100.0%	
> 3.850	50.00	23.66% to 76.34%	100.0	72.25% to 100.0%	
> 3.950	30.00	10.78% to 60.32%	100.0	72.25% to 100.0%	
> 4.150	20.00	3.554% to 50.98%	100.0	72.25% to 100.0%	
> 4.550	10.00	0.5129% to 40.42%	100.0	72.25% to 100.0%	

Fig. S6. Receiver Operating Characteristic (ROC) curve analysis for distinguishing NPDR vs PDR groups based on tear LCN-1 fluorescence intensity. The ROC curve was generated using GraphPad Prism software, with TP, FN, T), and FP classifications derived from clinical sample results. The highlighted yellow line indicates the optimal cut-off point selected by the software, corresponding to the highest combined sensitivity (100%) and specificity (90%). The calculated accuracy was 95% (19 correct classifications out of 20 samples).

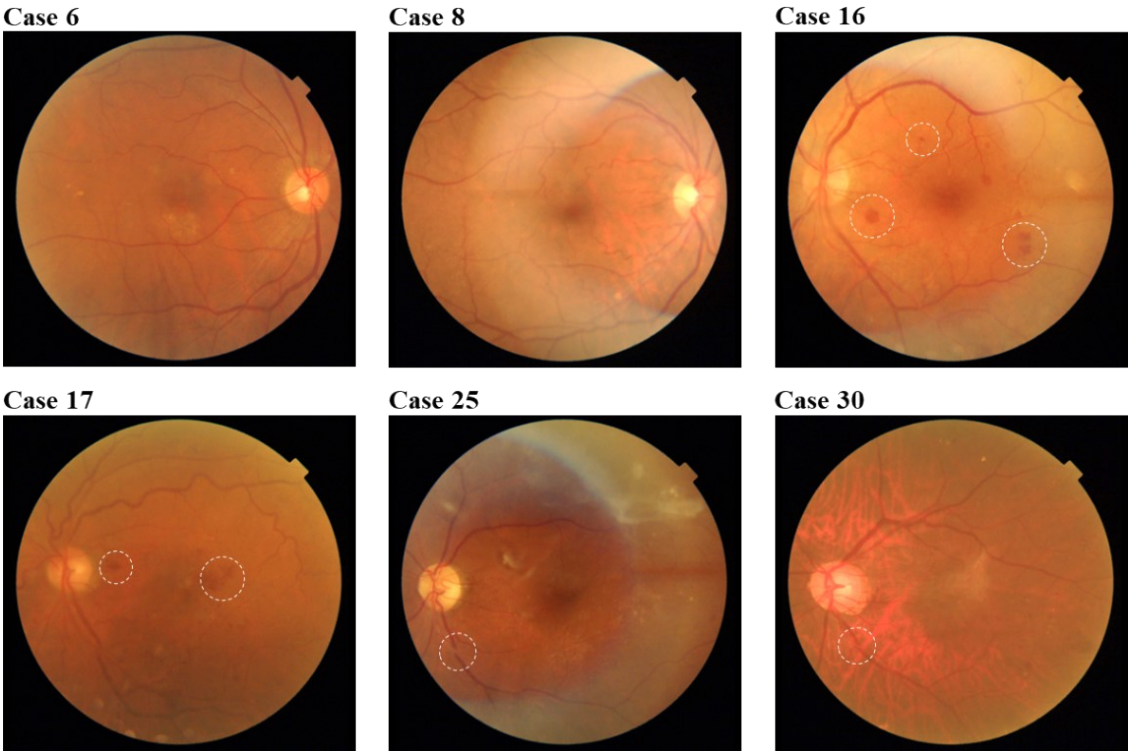

Fig. S7 Ophthalmoscopy images of test subjects of Healthy, NPDR and PDR patients. Labels correspond to patients 6 and 8 (healthy controls), patients 16 and 17 (non-proliferative diabetic retinopathy, NPDR), and patients 25 and 30 (proliferative diabetic retinopathy, PDR). The white dotted circles indicate hemorrhage in the PDR and NPDR cases.

Table S1: Photonics-Based Technologies for Tear Analyte Detection

Reference	Target Biomarker	Technology	Sensitivity (%)	Specificity (%)	Accuracy (%)	Limit of Detection
Realization of Rapid Diabetic Retinopathy Screening with Lipocalin 1 in Tear Using Enhanced Immunofluorescence Photonic Crystal Microchip (This work)	Lipocalin-1	Photonic Crystal Microchip	100	100	100	136 pg/μL
2D Photonic Crystal Hydrogel Sensor for Tear Glucose Monitoring[1]	Glucose	2D Photonic Crystal Hydrogel	NR	NR	NR	0.05 mM (~9 mg/L)
Photonic crystals: emerging biosensors and their promise for point-of-care applications[2]	Various proteins	Photonic Crystal Biosensor	90	95	92	NR
Contact lens as an emerging platform for non-invasive bio-sensing: A review[3]	Glucose	Optical Contact Lens	NR	NR	NR	NR
Graphene oxide-decorated hydrogel inverse opal photonic crystal improving colorimetric and fluorescent responses for rapid detection of lipocalin-1[4]	Lipocalin-1	GO-decorated hydrogel inverse opal photonic crystal	NR	NR	NR	≈ 0.06 mg/mL (mentioned, not explicitly stated as LoD)

"NR" = Not reported in the respective publication's main text or supplementary data.

Table S2: Other Technologies for Tear Analyte Detection

Reference	Target Biomarker	Technology	Sensitivity (%)	Specificity (%)	Accuracy (%)	Limit of Detection
Realization of Rapid Diabetic Retinopathy Screening with Lipocalin 1 in Tear Using Enhanced Immunofluorescence Photonic Crystal Microchip (This work)	Lipocalin-1	Photonic Crystal Microchip	100	100	100	136 pg/μL
Rapid tear screening of diabetic retinopathy by a detachable surface acoustic wave enabled immunosensor[5]	Lipocalin-1	Detachable SAW Microchip	NR	NR	NR	3 μg/mL
Microfluidic Immunosensor for Point-of-Care-Testing of Beta-2-Microglobulin in Tear[6]	β-2 microglobulin	Microfluidic Immunosensor	89	92	90	NR
An artificial intelligence-assisted microfluidic colorimetric wearable sensor system for monitoring of key tear biomarkers[7]	Protein Panel	AI Microfluidic Colorimetric	83.4	95.2	92.3	NR
Tear-based MMP-9 detection: A rapid antigen test for ocular inflammatory disorders using vanadium disulfide nanowires assisted chemi-resistive biosensor[8]	MMP-9	Rapid Antigen Test (LFA)	75	98	NR	NR
Paper integrated microfluidic contact lens for colorimetric glucose detection[9]	Glucose	Microfluidic Contact Lens Patch	NR	NR	NR	NR

"NR" = Not reported in the respective publication's main text or supplementary data.

Table S3. Patient Demographics, DR Status, HbA1c Levels, and Converted Biomarker Concentrations. PDR: proliferative diabetic retinopathy; NPDR: non-proliferative diabetic retinopathy; X: healthy control; HbA1c: glycated hemoglobin; ΔF: Relative fluorescence intensity, (-): data not available.

No.	Gender	Age	DR	Hba1c	ΔF	LCN-1 (mg/mL)
1	M	22	X	-	35.1	0.501
2	F	21	X	-	39.1	0.623
3	F	25	X	-	40.7	0.732
4	F	23	X	-	43.2	0.881
5	M	36	X	-	46.4	1.200
6	M	62	X	-	42.3	0.825
7	F	69	X	-	43.3	0.885
8	F	69	X	-	44.1	0.939
9	M	49	X	-	45.9	1.060
10	M	71	X	-	54.5	1.941
11	M	55	NPDR	6.6%	48.6	1.285
12	F	74	NPDR	6.2%	55.2	2.037
13	F	72	NPDR	8.3%	59.4	2.731
14	M	45	NPDR	10.1%	60.2	2.888
15	M	74	NPDR	7.5%	57.9	2.459
16	M	74	NPDR	7.6%	59.7	2.789
17	M	71	NPDR	-	58.9	2.637
18	F	65	NPDR	6.8%	57.4	2.375
19	F	66	NPDR	-	58.8	2.619
20	M	70	NPDR	7.0%	58.1	2.500
21	M	49	PDR	6.5%	60.3	2.908
22	M	62	PDR	7%	62.9	3.486
23	F	65	PDR	10%	64.2	3.817
24	M	56	PDR	8.8%	64.6	3.925
25	F	60	PDR	8.1%	64.7	3.953
26	M	67	PDR	6.3%	63.2	3.560
27	F	51	PDR	5.2%	62.5	3.391
28	M	63	PDR	6.2%	64.6	3.925
29	F	63	PDR	-	66.0	4.328
30	F	60	PDR	10.6%	67.5	4.806

Video S1: Fluid flow inside the microfluidic chip containing the absorbent paper of Design 3 (Playback speed: 60×).

References

1 C. Chen, Z.-Q. Dong, J.-H. Shen, H.-W. Chen, Y.-H. Zhu and Z.-G. Zhu, *ACS Omega*, 2018, **3**, 3211–3217.

2 H. Inan, M. Poyraz, F. Inci, M. A. Lifson, M. Baday, B. T. Cunningham and U. Demirci,
Chem. Soc. Rev., 2017, **46**, 366–388.
3 K. H. Shetty, D. T. Desai, H. P. Patel, D. O. Shah, M. D. P. Willcox and F. A. Maulvi, *Sensors and Actuators A: Physical*, 2024, **376**, 115617.
4 P. H. Phong, H.-S. Chuang, D. Thi Thuong, N. N. Sang, N. Thi Ha Lien, N. T. Nghia, N. D. Toan and L. M. Thanh, *Photonics and Nanostructures - Fundamentals and Applications*, 2024, **58**, 101237.
5 D. Das, H.-A. Chen, C.-L. Weng, Y.-C. Lee, S.-M. Hsu, J.-S. Kwon and H.-S. Chuang,
Analytica Chimica Acta, 2024, **1325**, 343117.
6 S. Maity, S. Ghosh, T. Bhuyan, D. Das and D. Bandyopadhyay, *ACS Sustainable Chem.*
Eng., 2020, **8**, 9268–9276.
7 Z. Wang, Y. Dong, X. Sui, X. Shao, K. Li, H. Zhang, Z. Xu and D. Zhang, *npj Flex Electron*, 2024, **8**, 35.
8 T. N. Ghosh, D. Rotake, S. Kumar, I. Kaur and S. G. Singh, *Analytica Chimica Acta*, 2023, **1263**, 341281.
9 P. K. Isgor, T. Abbasiasl, R. Das, E. Istif, U. C. Yener and L. Beker, *Sens. Diagn.*, 2024,
3, 1743–1748.